Improved tumor vascular function following high dose epidermal growth factor receptor tyrosine kinase inhibitor therapy

Mark M. Moasser, MD[1,3], **Lisa J. Wilmes, PhD**[2], **Ching Hang Wong, PhD**[1], **Sheye Aliu, BS**[2], **Ka-Loh Li, PhD**[2], **Donghui Wang, BS**[3], **Yun Kit Hom, PhD**[3], **Byron Hann, MD-PhD**[3], and **Nola M. Hylton, PhD**[2,3]

[1] Department of Medicine, University of California San Francisco, San Francisco, CA 94143

[2] Department of Radiology, University of California San Francisco, San Francisco, CA 94143

[3] Comprehensive Cancer Center, University of California San Francisco, San Francisco, CA 94143

Abstract

Purpose—To determine if inhibitors of the human growth factor receptor (HER) family can be used to enhance tumor vascular permeability and perfusion and optimize the efficacy of cytotoxic chemotherapeutics. Poor tumor vascular function limits the delivery and efficacy of cancer chemotherapeutics and HER family tyrosine kinases mediate tumor-endothelial signaling in both of these compartments.

Materials and Methods—BT474 human breast cancer tumors were established in mice and the biologic effects of the HER tyrosine kinase inhibitor (TKI) gefitinib on tumor vascular function was determined by dynamic contrast enhanced MRI (DCE-MRI), and on tumor vascular architecture and perfusion by immunofluorescence microscopy.

Results—A brief dose of gefitinib enhances the anti-tumor activity of paclitaxel *in vivo* but not in cell culture, suggesting that its chemo enhancing activity involves the *in vivo* micro-environment. A brief high dose of gefitinib induces a decrease in endothelial transfer constant Kps and a concomitant increase in tumor fractional plasma volume (fPV). These changes are accompanied by a rapid reduction in tumor volume likely due to decreased tumor edema, and modestly improved tumor vascular architecture and perfusion on microscopy.

Conclusion—These data suggest that HER family TKIs have the potential to optimize the tumor microenvironment for delivery of cytotoxic chemotherapeutics.

Keywords

Gefitinib; perfusion; chemotherapy; epidermal growth factor receptor; EGFR

Introduction

The treatment of solid tumor cancers is notoriously restricted by poor penetration of chemotherapeutic drugs into tumor tissues (reviewed in (1)). A major barrier to drug delivery is the structurally and functionally abnormal tumor vasculature. They are porous, disorganized, and dysfunctional, and result in an abnormal tumor microenvironment characterized by interstitial hypertension, hypoxia, and acidosis ((2) and reviewed in (3)).

Corresponding author: Mark M. Moasser, UCSF Box 0875, University of California, San Francisco, San Francisco, CA 94143, Tel: 415-476-0158, Fax: 415-502-5665, mmoasser@medicine.ucsf.edu.

These properties prevent efficient delivery of therapeutics to tumor cells. As such, there is considerable interest in developing adjunctive modalities to enhance the delivery of drugs into tumor tissues. Agents that target tumor endothelium have been at the forefront of this endeavor, in particular agents that target vascular endothelial growth factor (VEGF) signaling. Anti-VEGF therapies induce tumor vascular remodeling accompanied by functional changes that include decreased tumor interstitial fluid pressure and re-establishment of a hydrostatic pressure gradient across the normalized vascular wall which facilitates drug transport (4). Looking at albumin perfusion and diffusion into tumor tissues, Tong et al reported a significant decrease in albumin permeability across the tumor vascular walls after treatment with anti-VEGFR2 antibodies, but deeper penetration of albumin into tumor tissues (4). This treatment hypothesis has been supported by phase III clinical studies showing that the addition of anti-VEGF antibodies significantly improves the efficacy of chemotherapeutic agents in cancers of the breast, colon, and lung (5–7).

Dynamic contrast enhanced MRI (DCE-MRI) using macromolecular contrast media with pharmacokinetic modeling has proven highly instrumental in characterizing and confirming the functional changes in tumor vasculature, in particular trans-endothelial permeability, following treatment with vascular targeting drugs. Elevated Kps is a pathologic feature of hyperpermeable tumor vasculature since it is not usually seen in benign lesions, but frequently seen in malignant tumors (8). Studies by us and other groups using DCE-MRI in preclinical models confirm that several classes of agents that target VEGF signaling induce a reduction in tumor trans-endothelial permeability (Kps) (9–14). These effects are evident as early as 24 hours of treatment in some models.

Tumor vasculature is also regulated by signaling pathways other than the VEGF receptors and these alternate pathways can potentially be targeted to enhance vascular function. The human epidermal growth factor receptor (HER) family of tyrosine kinases (TKs) are widely expressed in adult tissues and signal diverse cellular functions including proliferation, differentiation, metabolic functions and cell survival. When deregulated in certain cancers, HER kinases promote uncontrolled growth, invasiveness, hypermetabolism and anti-apoptotic attributes (15). HER kinases also mediate some of the angiogenic properties of cancer cells (16,17). Importantly, HER kinases are involved in angiogenic signaling both within tumor cells through regulation of VEGF expression, and within endothelial cells through regulation of Akt signaling (18–22). This suggests that inhibitors of HER TKs may target both the tumor and microenvironment compartments and may have enhanced ability to improve tumor vascular function.

HER TKIs can enhance the anti-tumor effects of chemotherapeutic agents in preclinical models (23,24). But this effect is modest in preclinical models and is not seen in phase III clinical studies (25,26). Recent evidence suggests that Akt-driven feedback signaling through HER3 significantly attenuates the effects of TKIs and much higher potency or high dose TKIs are required to effectively suppress HER family signaling (27). This intrinsic resistance is overcome by use of HER TKIs at high dosages and has significant implications for the future use of these agents. The clinical use of TKIs at high doses given daily is impractical due to their dose-limiting toxicities. However when used as chemosensitizers, they need not be used in continuous daily dosing. For this purpose they can be used in a brief one or two day dose which is more tolerable and allows higher doses to be administered. The brief but higher dose can be administered immediately prior to chemotherapy optimizing their use as chemosensitizers. The higher dose also allows better penetration of the TKI into tumor tissues and inactivation of targets within tumor cells and tumor vasculature, optimally priming the microenvironment for chemotherapeutic delivery. In this paper we report the effects of the HER TKI gefitinib on tumor vascular function by dynamic contrast enhanced MRI (DCE-MRI.). We compare the effects of a brief high dose

with a lower continuous dose and find highly favorable improvements in tumor vascular function in the time period immediately following a high dose, but not with continuous low dose therapy. These effects include a transient reduction in tumor Kps accompanied by an increase in fPV and slight decrease in tumor volume immediately following the pulse high dose of gefitinib. The favorable effects of high dose gefitinib on chemodelivery are corroborated by tumor growth studies and by fluorescence microscopic analysis of tumor sections.

Methods

Cell culture and cell based assays

Human BT474 breast cancer cells were obtained from the American Type Culture Collection (ATCC) and maintained in RPMI media supplemented with 100 U/ml penicillin, 100µg/ml streptomycin, 4mM glutamine, and 10% fetal bovine serum and incubated at 37 C in 5%CO_2. A highly tumorigenic subline of the parental BT474 cells were used in this study. For assays of apoptosis, cells were seeded in 10cm dishes and the following day treated with the indicated drugs for 24 hours. Cells were then collected by trypsinization and analyzed for Annexin V binding using the Invitrogen kit according to manufacturers' protocol. Annexin V binding is widely used to identify apoptotic cells. The percentage of cells binding Annexin V was quantified by flow assisted cell sorter (FACS) analysis counting 20,000 events.

Animal anti-tumor studies

NCR nu/nu mice pre-implanted with estrogen pellets (0.72ug, Innovative Research) were injected subcutaneously with 10 million tumor cells and allowed to grow until approximately 200–300 mm^3 in size. At that time mice were randomized into the indicated treatment arms. In these experiments, gefitinib is administered at its maximal tolerated dose (MTD) in the continuously dosed and pulsed arms in order to most effectively predict how these schedules would compare in clinical scenarios. The MTD for gefitinib when given as a two day dose preceding weekly paclitaxel is 250 mg/kg which is more than four times higher than the MTD of 60 mg/kg when given every day along with weekly paclitaxel. The paclitaxel alone group received paclitaxel 30 mg/kg administered intraperitoneally (IP) once per week for three weeks. All other paclitaxel containing arms received the same dose and schedule of paclitaxel. Gefitinib was administered at the maximum tolerated dose in each of the gefitinib combination arms. The daily gefitinib alone group received gefitinib once per day by oral gavage at 150 mg/kg. The daily gefitinib and paclitaxel group received gefitinib at 60 mg/kg. The pulse gefitinib and paclitaxel group received gefitinib for two days prior to paclitaxel at 250 mg/kg. The control group received daily vehicle (PBS-tween) by oral gavage. Animals were monitored daily and tumors measured by calipers twice per week.

MRI studies

For imaging studies, mice were implanted with BT474 cells and tumors were allowed to grow to approximately 100 mm^3. Mice were selected for MRI studies from a larger cohort of tumor-bearing mice, size-matched and randomly assigned to the experimental arms. Mice were treated according to three arms of 5–6 mice each. In the continuous treatment arm, mice were treated with daily gefitinib at a daily dose of 150 mg/kg. In the pulse treated arm, mice were treated with two days of gefitinib at 1000 mg/kg. The pulsed gefitinib arm was dosed high to allow the detection of subtle, but functionally important, effects below the sensitivity of MRI. Control mice were treated with vehicle carrier. All treatments were by oral gavage. MRIs were obtained at three timepoints in all experimental arms. These were at baseline, and again on day 3, and on day 8 (see schematic, figure 3A). Mice were imaged in pairs in a clinical MRI scanner using a wrist radiofrequency coil (Medical Advances,

Milwaukee, WI). The mice were anesthesized by inhalation with 1.5% isoflurane administered via an MR-compatible mobile inhalation anesthesia system (Vet Equip, Pleasanton, CA). The tail vein was cannulated before the mice were placed in the magnet for contrast medium injection during MRI. MRI was performed on a 1.5T Signa whole body MRI scanner (General Electric Medical Systems, Milwaukee, WI). Precontrast tissue T_1 (T_{10}) was measured using a 3D variable flip angle fast gradient-echo technique (28). DCE-MRI was performed using a T1-weighted 3D gradient-echo sequence (TR=10.2 msec, TE=4.2 msec, FA=20°, FOV=10×10cm, imaging matrix=256×192, slice thickness=1.0mm, NEX=1) with a time resolution of 63 seconds over a period of 48 minutes. Five precontrast scans were acquired before the mice were injected via the tail vein with 0.03 mmol/kg albumin-(Gd-DPTA)$_{30}$ in a volume of 100 ul (29).

Quantitative analysis of albumin-(Gd-DTPA)$_{30}$ enhanced MR imaging data was based on a two-compartment, unidirectional pharmacokinetic model, which assumes no reflux of the macromolecular contrast material (MMCM) from the tumor interstitium into the vascular compartment during the time course of the imaging experiment (30,31). Details regarding the pharmacokinetic analysis of the DCE MRI data have been previously described (9). In brief, the time course of the intravascular contrast agent (CA) concentration measured from the abdominal aorta (or vena cava) was fit to a mono-exponential model, producing an effective vascular input function (VIF) for each examination. Lesion boundaries were assigned manually in the DCE MRI images. The endothelial transfer constant Kps (ml/min/100ml tissue) and the fractional plasma volume fPV were estimated on a pixel-by-pixel basis for the regions of interest (ROIs) encompassing the entire tumor. A map of scaled fitting error (SFE) (9,32) was generated as an integral part of each fitting procedure to assess the discrepancy between the derived curve and the original data. Estimation of the tumor volume and the statistical analysis included all voxels within the tumor boundaries that fell into the following criteria: 1) voxel associated with a good fit to the model (SFE < 50%); 2) voxel with the fPV value within the physiological range of a living tissue ($0 < fPV < 0.5$). Voxels, which did not meet the above criteria, were omitted, i.e., the value of the Kps and fPV were set to zero and excluded from the tumor volume estimation and the statistical analysis. The SFE threshold value of 0.5 was empirically determined according to the overall signal to noise ratio (SNR) in the DCE MRI data being analyzed.

Lectin perfusion studies

Mice bearing 100 mm^3 BT474 tumors were treated with 1000 mg/kg gefitinib or vehicle for 2 days and the histologic analyses were conducted on the third day. The third day corresponds to the timepoint of the MRI studies and the time point of paclitaxel administration in the other experiments described here. Four gefitinib treated and four control mice were studied. For this analysis, mice were anesthetized and administered 100 μg of fluorescein isothiocyanate (FITC)-labeled lectin (Vector Labs, Burlingame, CA) in 0.9% NaCl (100 μl) by tail vein injection (33). Two minutes later the chest was opened rapidly, and the vasculature was perfused for 2 min at a pressure of 120 mmHg with fixative (1% paraformaldehyde in phosphate buffered saline (PBS), pH 7.4, Sigma, St. Louis, MO) from an 18-gauge cannula inserted into the aorta via an incision in the left ventricle. Blood and fixative exited through an opening in the right atrium.

After fixation by vascular perfusion, organs and tumors were removed, rinsed several times with PBS, infiltrated with 30% sucrose, and frozen in OCT compound. 80 uM cryostat sections were permeabilized and incubated in 5% normal serum in PBS-T (containing 0.3% Triton X-100, 0.2% bovine serum albumin (Sigma), and 0.01% thimerosal (Sigma)) for 1 hr at room temperature to block non-specific antibody binding. Sections were incubated with anti-CD31 antibodies (PECAM-1, clone MEC 13.3, 1:1000, Pharmingen, San Diego, CA) in 5% serum in PBS-T overnight at room temperature. Sections were stained with secondary

anti-rat Cy3 antibodies, rinsed with PBS-T, fixed in 4% paraformaldehyde, rinsed again with PBS, and mounted in Vectashield (Vector Laboratories, Burlingame, CA). Sections were examined under fluorescence microscopy using appropriate filters.

Results

Mice bearing BT474 breast cancer xenograft tumors were treated with the chemotherapeutic agent paclitaxel and the HER family TKI gefitinib in different schedules. In this tumor model, the addition of continuously dosed gefitinib at its maximum tolerated dose to paclitaxel does not enhance the anti-tumor effects of paclitaxel significantly (figure 1, compare arms B & D). However, when gefitinib is given just two days prior to paclitaxel, much higher doses can be delivered, and the anti-tumor efficacy of paclitaxel is enhanced (figure 1, compare arms D & E). A two day pulse of gefitinib is only effective if given preceding paclitaxel, but not following paclitaxel (not shown). The beneficial effects of a gefitinib pulse preceding the paclitaxel are not just due to the higher gefitinib pulse dose, since this effect is not apparent in the control arm that received the same dose gefitinib pulse without paclitaxel (figure 1, compare arms E & F).

Paclitaxel is a cytotoxic chemotherapeutic agent and induces a dose-dependent pro-apoptotic effect on tumor cells. However the addition of gefitinib does not enhance the pro-apoptotic effects of paclitaxel on tumor cells including BT474 cells (figure 2). No enhancement of paclitaxel induced apoptosis is seen whether gefitinib is administered prior to or concomitant with paclitaxel or at concentrations up to 50 uM (figure 2 and data not shown). Therefore the gefitinib-induced paclitaxel sensitization that we see *in vivo* must involve mechanisms that involve the *in vivo* microenvironment. We hypothesized that gefitinib induces changes in tumor vascular function, in particular permeability characteristics, that enhance the *in vivo* potency of paclitaxel. To study this hypothesis we studied the effects of gefitinib on tumor microvascular function by dynamic contrast enhanced MRI (DCE-MRI).

DCE-MRI using macromolecular contrast agents is particularly well suited for studying tumor vasculature as their minimal leakage from normal vessels and their prolonged intravascular retention makes them particularly well suited for studying tumor vascular hyper-permeability characteristics. A two day pulse of gefitinib treatment produces a transient but significant reduction in the endothelial transfer constant (Kps) that returns to baseline by day 8 (figure 3B). A similar reduction in Kps is not seen with the lower continuous dosing of gefitinib. In addition, the two day pulse of gefitinib results in a transient increase in tumor fractional plasma volume (fPV), a measure of tumor perfusion (figure 3C). The increase in fPV seen immediately following the 2 day pulse of gefitinib returns to baseline by day 8. Continuous gefitinib treatment also produces a gradual increase in fPV over the same time period (figure 3C). Tumor in control mice show no clear evidence of changes in Kps or fPV in this analysis.

Analysis of tumor volumes reveals an unexpected and interesting finding in pulse-gefitinib treated tumors. There is a small reduction in tumor volume immediately following two days of a gefitinib pulse (figure 3D). This is not due to tumor cell death since gefitinib is cytostatic and does not cause tumor cell death in monolayer models (figure 2), and there is no evidence of rapid tumor cell death by microsopic analysis of tumors from pulse treated mice (data not shown). The transient volume reduction seen on day 3 following the gefitinib pulse is likely due to reduced tumor interstitial edema resulting from improved tumor vascular hemodynamics and is consistent with the transient reduction in Kps combined with the transient increase in fPV at this timepoint.

Next we studied tumor vascular architecture and perfusion by fluorescence microscopy using lectin-perfusion experiments. Lectin introduced into the vascular lumen stains the vascular endothelium upon contact and the analysis of green fluorescence after intravenous lectin-FITC injection identifies the vasculature that was succesfully perfused following the intraveneous administration of the FITC-labeled lectin. Anti-CD31 antibodies also stain endothelial cells and staining tissue sections with anti-CD31 identifies all vasculature regardless of blood flow and perfusion characterstics. Therefore anti-CD31 stains the entire vasculature and provides architectural information, while lectin-FITC perfusion stains only the perfused vasculature and provides functional information that identifies the fraction of the vasculature that is well perfused. Microscopic analysis shows that BT474 tumors grown subcutaneously in mice have poor vascular perfusion (figure 4A). This is typical of many xenograft models and tumor growth in general, and is not an artifact of poor lectin perfusion of the mice, since analysis of sections from kidney and other organs shows good lectin-FITC staining (data not shown). Comparing tumors from gefitinib treated and untreated mice shows improved tumor vascular architecture and modestly increased lectin perfusion in gefitinib treated mice (figure 4B).

Discussion

We report, for the first time, the effect of a HER family TKI on tumor vascular function. While the effects of inhibitors of VEGF signaling have been extensively studied and reported, other signaling pathways are also involved in regulating endothelial cell signaling and tumor-endothelial cross-talk. The HER family of receptor tyrosine kinases are an important family of signaling molecules that are known to be involved in endothelial cell signaling, critically involved in many human tumors, and also involved in cross-talk with VEGF signaling. We report here that high dose HER TKI gefitinib can be used to induce a transient reduction in tumor Kps and a transient increase in fPV. These characteristics result in a transient reduction in tumor volume that is consistent with reduced intersitial fluid and likely reduced tissue hypertension, all of which create a micro-environment favorable for the delivery of cytotoxic chemotherapy.

While our finding of decreased Kps mimics the data from VEGF targeted therapies, our finding of increased fPV following gefitinib treatment is unlike the observations made with VEGF targeted therapies. In several studies of VEGFR inhibitors fPV was either unchanged or reduced following treatment (9–12,14,34). Ours is the first study using DCE-MRI to assess tumor perfusion following HER TKIs and the finding of increased fPV suggests that this class of inhibitors may have vascular characteristics that are distinct from VEGF targeting agents. The increased perfusion suggested by increased fPV and histologic analysis, combined with improved endothelial wall pressure gradients suggested by the reduced Kps may improve chemodelivery even more effectively than VEGF targeted therapies. Gefitinib could increase tumor fPV by increasing flow, either through direct effects on vascular tone, or through relief from the compressive effects of tissue hypertension. Increased tumor blood flow has been seen with agents that relax tumor vascular tone by targeting the endothelin receptor in tumor arterioles (35). While increased flow alone, as with endothelin antagonists, could lead to increased tissue hydrostatic pressure and increased tumor volume (35), the combination of increased flow and decreased capillary permeabilty as seen with gefitinib could establish characteristics that most effectively reverse the pathologic attributes of tumor vasculature, and re-establish more physiologic efferent and afferent trans-endothelial exchange of fluids and solutes. The reduced tumor volume that we see following a pulse of gefitinib treatment is suggestive of reduced tumor edema and is consistent with such a model. Increased fPV could also reflect a stable plasma volume and stable flow but could be secondary to a reduction in extracellular fluid volume. A reduction in the extracellular tumor volume and total tumor volume (which

we observe) would lead to a relative increase in the fractional plasma volume (fPV) that we see.

The molecular mechanisms by which HER TKIs suppress tumor vascular permeability have not directly been studied. In tumor cells, HER signaling induces a transcriptional program leading to the expression of a number of angiogenic factors (36), and specifically induces the expression and secretion of vascular endothelial growth factor (VEGF) through pathways that include mTOR and HIF-1 (18,19), and the expression and activity of angiogenic matrix metalloproteinases (37). In endothelial cells, HER kinases promote angiogenic signaling that is independent of VEGF signaling (38,39). These angiogenic effects are mediated through downstream Akt signaling (20,21). Since Akt signaling also mediates permeability characteristics in endothelial cells (40,41), HER signaling may also partially regulate endothelial permeability through its ability to regulate Akt.

These studies suggest a novel approach to enhance the efficacy of chemotherapeutics using HER TKIs and the potential of DCE-MRI to monitor this activity during clinical translation.

Acknowledgments

Reference List

1. Minchinton AI, Tannock IF. Drug penetration in solid tumours. Nat Rev Cancer 2006;6:583–592. [PubMed: 16862189]

2. Padera TP, Stoll BR, Tooredman JB, Capen D, di TE, Jain RK. Pathology: cancer cells compress intratumour vessels. Nature 2004;427:695. [PubMed: 14973470]

3. Jain RK. Normalization of tumor vasculature: an emerging concept in antiangiogenic therapy. Science 2005;307:58–62. [PubMed: 15637262]

4. Tong RT, Boucher Y, Kozin SV, Winkler F, Hicklin DJ, Jain RK. Vascular normalization by vascular endothelial growth factor receptor 2 blockade induces a pressure gradient across the vasculature and improves drug penetration in tumors. Cancer Research 2004;64:3731–37336. [PubMed: 15172975]

5. Miller KD, Wang M, Dickler M, Cobleigh MA, Perez EA, Shenkier TN, Davidson NE. A randomized phase III trial of paclitaxel versus paclitaxel plus bevacizumab as first-line therapy for locally recurrent or metastatic breast cancer: a trial coordinated by the Eastern Cooperative Oncology Group (E2100). Proc San Antonio Br Can Symp 2005:3.

6. Sandler AB, Gray R, Brahmer J, Dowlati A, Schiller JH, Perry MC, Johnson DH. Randomized phase II/III Trial of paclitaxel (P) plus carboplatin (C) with or without bevacizumab (NSC # 704865) in patients with advanced non-squamous non-small cell lung cancer (NSCLC): An Eastern Cooperative Oncology Group (ECOG) Trial - E4599. Proc Amer Soc Clin Onc 2005:4.

7. Hurwitz HI, Fehrenbacher L, Hainsworth JD, et al. Bevacizumab in combination with fluorouracil and leucovorin: an active regimen for first-line metastatic colorectal cancer. J Clin Oncol 2005;23:3502–3508. [PubMed: 15908660]

8. Daldrup-Link HE, Rydland J, Helbich TH, et al. Quantification of breast tumor microvascular permeability with feruglose-enhanced MR imaging: initial phase II multicenter trial. Radiology 2003;229:885–892. [PubMed: 14576446]

9. Li KL, Wilmes LJ, Henry RG, et al. Heterogeneity in angiogenic response of BT474 human breast cancer to a novel vascular endothelial growth factor-receptor tyrosine kinase inhibitor: assessment by voxel analysis of dynamic contrast-enhanced MRI. Journal of Magnetic Resonance Imaging 2005;22:511–519. [PubMed: 16161072]

10. Marzola P, Degrassi A, Calderan L, et al. Early antiangiogenic activity of SU11248 evaluated in vivo by dynamic contrast-enhanced magnetic resonance imaging in an experimental model of colon carcinoma. Clin Cancer Res 2005;11:5827–5832. [PubMed: 16115922]

11. Pradel C, Siauve N, Bruneteau G, et al. Reduced capillary perfusion and permeability in human tumour xenografts treated with the VEGF signalling inhibitor ZD4190: an in vivo assessment using dynamic MR imaging and macromolecular contrast media. Magnetic Resonance Imaging 2003;21:845–851. [PubMed: 14599534]

12. Pham CD, Roberts TP, van BN, et al. Magnetic resonance imaging detects suppression of tumor vascular permeability after administration of antibody to vascular endothelial growth factor. Cancer Investigation 1998;16:225–230. [PubMed: 9589031]

13. Checkley D, Tessier JJ, Kendrew J, Waterton JC, Wedge SR. Use of dynamic contrast-enhanced MRI to evaluate acute treatment with ZD6474, a VEGF signalling inhibitor, in PC-3 prostate tumours. British Journal of Cancer 2003;89:1889–1895. [PubMed: 14612898]

14. Turetschek K, Preda A, Floyd E, et al. MRI monitoring of tumor response following angiogenesis inhibition in an experimental human breast cancer model. Eur J Nucl Med Mol Imaging 2003;30:448–455. [PubMed: 12722742]

15. Yarden Y. The EGFR family and its ligands in human cancer. signalling mechanisms and therapeutic opportunities. European Journal of Cancer 2001;37 (Suppl 4):S3–S8. [PubMed: 11597398]

16. Ellis LM. Epidermal growth factor receptor in tumor angiogenesis. Hematology - Oncology Clinics of North America 2004;18:1007–1021.

17. Kumar R, Yarmand-Bagheri R. The role of HER2 in angiogenesis. Seminars in Oncology 2001;28:27–32. [PubMed: 11706393]

18. Klos KS, Wyszomierski SL, Sun M, et al. ErbB2 increases vascular endothelial growth factor protein synthesis via activation of mammalian target of rapamycin/p70S6K leading to increased angiogenesis and spontaneous metastasis of human breast cancer cells. Cancer Res 2006;66:2028–2037. [PubMed: 16489002]

19. Laughner E, Taghavi P, Chiles K, Mahon PC, Semenza GL. HER2 (neu) signaling increases the rate of hypoxia-inducible factor 1alpha (HIF-1alpha) synthesis: novel mechanism for HIF-1-mediated vascular endothelial growth factor expression. Mol Cell Biol 2001;21:3995–4004. [PubMed: 11359907]

20. Shiojima I, Walsh K. Role of Akt signaling in vascular homeostasis and angiogenesis. Circ Res 2002;90:1243–1250. [PubMed: 12089061]

21. Dimmeler S, Zeiher AM. Akt takes center stage in angiogenesis signaling. Circ Res 2000;86:4–5. [PubMed: 10625297]

22. Kim HS, Shin HS, Kwak HJ, Cho CH, Lee CO, Koh GY. Betacellulin induces angiogenesis through activation of mitogen-activated protein kinase and phosphatidylinositol 3′-kinase in endothelial cell. FASEB Journal 2003;17:318–320. [PubMed: 12475887]

23. Ciardiello F, Caputo R, Bianco R, et al. Antitumor effect and potentiation of cytotoxic drugs activity in human cancer cells by ZD-1839 (Iressa), an epidermal growth factor receptor-selective tyrosine kinase inhibitor. Clinical Cancer Research 2000;6:2053–2063. [PubMed: 10815932]

24. Sirotnak FM, Zakowski MF, Miller VA, Scher HI, Kris MG. Efficacy of cytotoxic agents against human tumor xenografts is markedly enhanced by coadministration of ZD1839 (Iressa), an inhibitor of EGFR tyrosine kinase. Clinical Cancer Research 2000;6:4885–4892. [PubMed: 11156248]

25. Herbst RS, Giaccone G, Schiller JH, et al. Gefitinib in combination with paclitaxel and carboplatin in advanced non-small-cell lung cancer: a phase III trial--INTACT 2. J Clin Onc 2004;22:785–794.

26. Giaccone G, Herbst RS, Manegold C, et al. Gefitinib in combination with gemcitabine and cisplatin in advanced non-small-cell lung cancer: a phase III trial--INTACT 1. J Clin Onc 2004;22:777–784.

27. Sergina NV, Rausch M, Wang D, et al. Escape from HER family tyrosine kinase inhibitor therapy by the kinase inactive HER3. Nature 2007;445:437–441. [PubMed: 17206155]

28. Zhu X, Li KL, Waterton JC, et al. 3D T1 Mapping by Means of Fast Field Echo Technique. Proc Intl Soc Magnetic Resonance in Medicine 1999:2143.

29. Turetschek K, Preda A, Novikov V, et al. Tumor microvascular changes in antiangiogenic treatment: assessment by magnetic resonance contrast media of different molecular weights. J Magn Reson Imaging 2004;20:138–144. [PubMed: 15221819]

30. Patlak CS, Blasberg RG, Fenstermacher JD. Graphical evaluation of blood-to-brain transfer constants from multiple-time uptake data. Journal of Cerebral Blood Flow & Metabolism 1983;3:1–7. [PubMed: 6822610]

31. Turetschek K, Floyd E, Shames DM, et al. Assessment of a rapid clearance blood pool MR contrast medium (P792) for assays of microvascular characteristics in experimental breast tumors with correlations to histopathology. Magn Reson Med 2001;45:880–886. [PubMed: 11323815]

32. Li KL, Zhu XP, Jackson A. Parametric mapping of scaled fitting error in dynamic susceptibility contrast enhanced MR perfusion imaging. Br J Radiol 2000;73:470–481. [PubMed: 10884742]

33. Hashizume H, Baluk P, Morikawa S, et al. Openings between defective endothelial cells explain tumor vessel leakiness. Am J Pathol 2000;156:1363–1380. [PubMed: 10751361]

34. Marzola P, Degrassi A, Calderan L, et al. In vivo assessment of antiangiogenic activity of SU6668 in an experimental colon carcinoma model. Clin Cancer Res 2004;10:739–750. [PubMed: 14760097]

35. Martinive P, De WJ, Bouzin C, et al. Reversal of temporal and spatial heterogeneities in tumor perfusion identifies the tumor vascular tone as a tunable variable to improve drug delivery. Mol Cancer Ther 2006;5:1620–1627. [PubMed: 16818522]

36. Beckers J, Herrmann F, Rieger S, et al. Identification and validation of novel ERBB2 (HER2, NEU) targets including genes involved in angiogenesis. Int J Cancer 2005;114:590–597. [PubMed: 15609325]

37. Ongusaha PP, Kwak JC, Zwible AJ, et al. HB-EGF is a potent inducer of tumor growth and angiogenesis. Cancer Res 2004;64:5283–5290. [PubMed: 15289334]

38. Russell KS, Stern DF, Polverini PJ, Bender JR. Neuregulin activation of ErbB receptors in vascular endothelium leads to angiogenesis. American Journal of Physiology 1999;277:H2205–H2211. [PubMed: 10600838]

39. Vinci MC, Visentin B, Cusinato F, Nardelli GB, Trevisi L, Luciani S. Effect of vascular endothelial growth factor and epidermal growth factor on iatrogenic apoptosis in human endothelial cells. Biochemical Pharmacology 2004;67:277–284. [PubMed: 14698040]

40. Six I, Kureishi Y, Luo Z, Walsh K. Akt signaling mediates VEGF/VPF vascular permeability in vivo. FEBS Letters 2002;532:67–69. [PubMed: 12459464]

41. Lal BK, Varma S, Pappas PJ, Hobson RW, Duran WN. VEGF increases permeability of the endothelial cell monolayer by activation of PKB/akt, endothelial nitric-oxide synthase, and MAP kinase pathways. Microvascular Research 2001;62:252–262. [PubMed: 11678628]
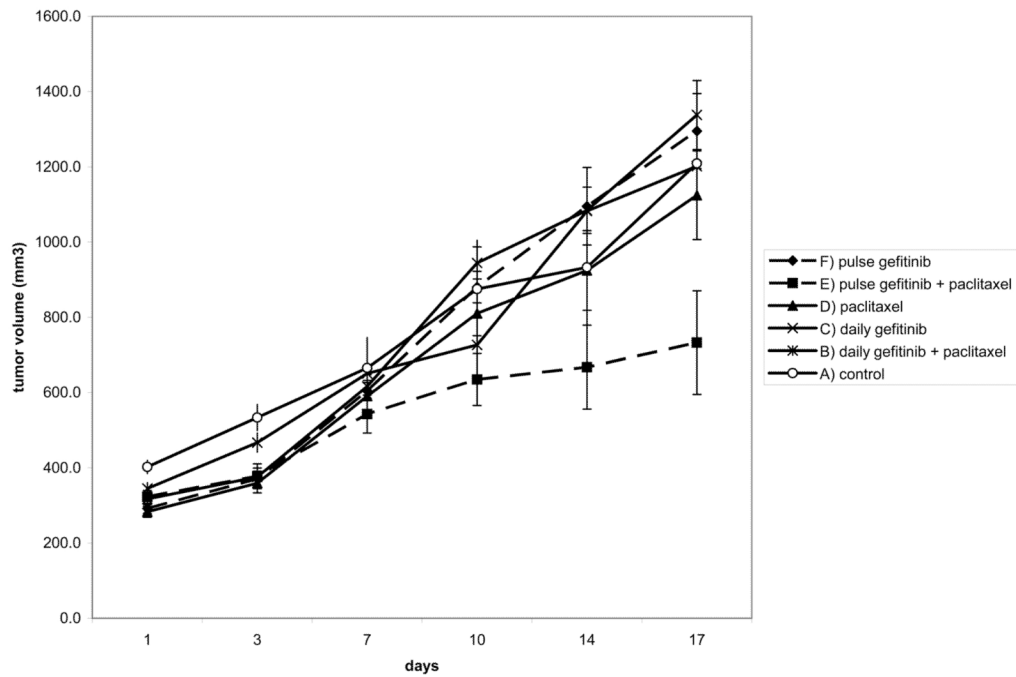
Figure 1.
60 mice bearing equal sized BT474 tumors were randomized into 6 groups and treated according to 6 treatment arms as indicated. Paclitaxel was administered at the fixed standard dose of 30 mg/kg given once per week. **A)** control arm received vehicle oral gavage daily, **B)** daily gefitinib+paclitaxel arm received gefitinib at 60 mg/kg daily. This is the MTD for daily gefitinib in this combination. **C)** Single agent daily gefitinib arm received gefitinib at 150 mg/kg daily. This is the MTD for single agent gefitinib. **D)** Paclitaxel alone arm received vehicle oral gavage daily. **E)** pulse gefitinib+paclitaxel arm received gefitinib for two days each week at 250 mg/kg followed by paclitaxel on the third day. This is the MTD for gefitinib in this combination. **F)** The pulse gefitinib alone arm received gefitinib for two days each week at 250 mg/kg. This arm is a no-paclitaxel control for arm E.
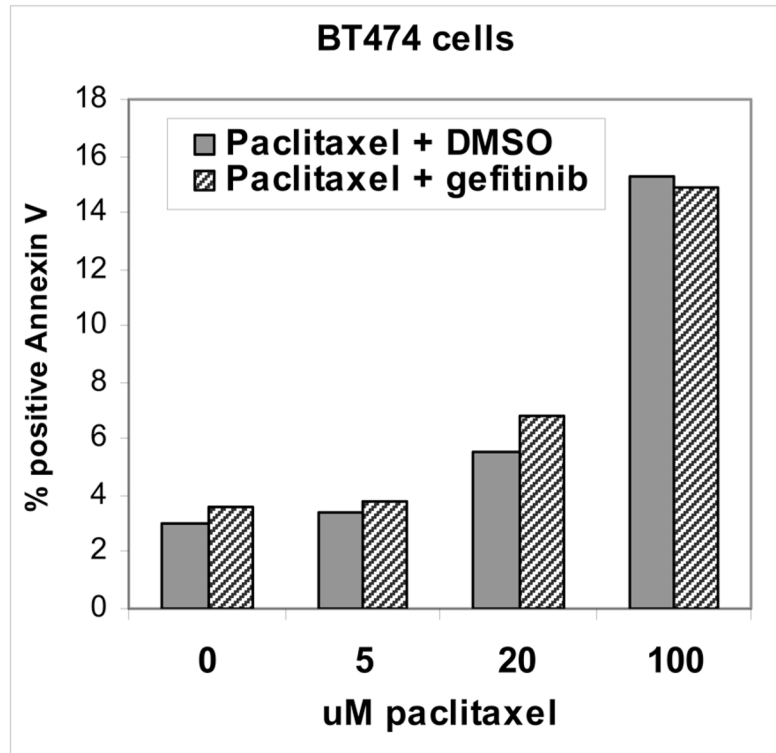
Figure 2.
BT474 cells were seeded in 10cm dishes and the following day treated with the indication
concentrations of paclitaxel concomitantly with 5uM gefitinib or DMSO (dimethyl
sulfoxide) vehicle control. After 24 hours, cells were harvested and apoptotic cells were
identified and quantitated by FACS analysis of annexin V binding as described in methods.
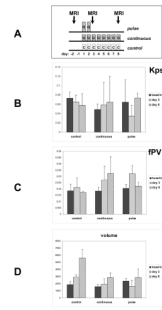Annexin V binding identifies apoptotic cells.

Figure 3.
Mice bearing BT474 tumors of approximately equal size were treated according to 3 treatment arms. A) A schematic displaying the treatments administered in the three arms. The pulse-treatment arm consisted of 6 mice receiving gefitinib for only two days at 1000 mg/kg/day. The continuous-treatment arm consisted of 6 mice receiving gefitinib daily at 150 mg/kg/day. The control arm consisted of four mice receiving vehicle by oral gavage. All mice underwent DCE-MRI studies at baseline and on day 3 and on day 8 as depicted. B) Transendothelial permeability (Kps) values were calculated for each of the three treatment arms at the three studied timepoints. Y axis reflects Kps in ml/100g/min. B) Fractional plasma volume (fPV) was calculated for each of the three treatment arms at the three studied timepoints. Y axis reflects fPV as a fraction of 1. C) Tumor volume in voxel numbers is shown for each of the three treatment arms at the three studied timepoints. Error bars; SD.
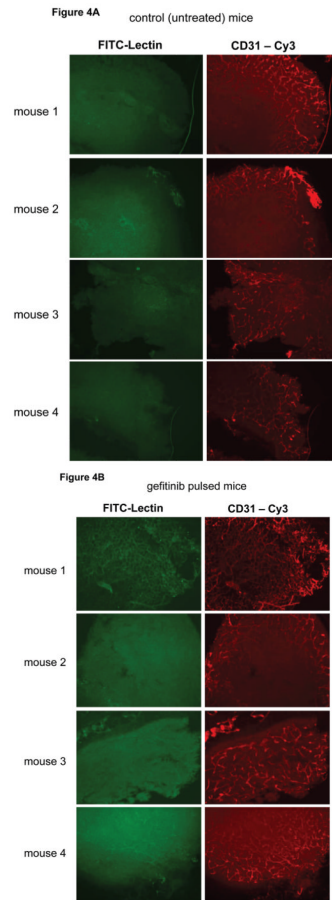
Figure 4.
Eight mice bearing BT474 tumors of approximately equal size were divided into two groups and treated with 1000 mg/kg gefitinib for two days or control gavage and on the third day the tumor vasculature was studied by lectin-perfusion *in vivo* staining and by anti-CD31 immunostaining of tumor sections as described in methods. Lectin perfusion staining is in green; anti-CD31 staining is in red.